

Critical dynamics of an isothermal non-ideal fluid

Markus Gross^{1,*} and Fathollah Varnik^{1,2}

¹*Interdisciplinary Centre for Advanced Materials Simulation (ICAMS),
Ruhr-Universität Bochum, Universitätsstr. 90a, 44789 Bochum, Germany*

²*Max-Planck Institut für Eisenforschung, Max-Planck Str. 1, 40237 Düsseldorf, Germany*

A pure fluid at its critical point shows dramatic slowing down in its dynamics, owing to a divergence of the order-parameter susceptibility and the coefficient of heat transport. Under isothermal conditions, however, sound waves provide the only possible relaxation mechanism for order-parameter fluctuations. Here, we study the critical dynamics of an isothermal, compressible non-ideal fluid via scaling arguments and computer simulations of the corresponding fluctuating hydrodynamics equations. We show that, below a critical dimension of 4, the order-parameter dynamics of an isothermal fluid effectively reduces to “model A”, characterized by overdamped sound waves and a divergent bulk viscosity. In contrast, the shear viscosity remains finite above two dimensions. Possible applications of the model to monolayer films are discussed.

I. INTRODUCTION

The presence of long-range static correlations can induce drastic slowing down of the dynamics of a fluid at the critical point [1, 2]. This can be understood by noting that the order-parameter relaxation rate is typically given as a ratio between a transport coefficient and a susceptibility: the susceptibility diverges critical point, while the transport coefficient remains roughly constant (or has a much weaker divergence). The characteristic dependence of the relaxation rate Γ on the wavenumber, $\Gamma \propto k^z$, or, by virtue of the dynamic scaling assumption, equivalently on the correlation length, $\Gamma \propto \xi^{-z}$, defines the *dynamic critical exponent* of the order parameter, z . In addition to the order-parameter relaxation time, other transport coefficients of a fluid, such as the viscosity, are often divergent as well and entail their own critical exponents. Similarly to statics, many properties of dynamic critical fluctuations, such as dynamic critical exponents or amplitude ratios, are universal and thus not specific to a particular substance. For instance, an energy-conserving pure (i.e., single-component) fluid at the liquid-vapor critical point and a binary fluid at the demixing point both belong to the same dynamic universality class of *model H* and thus share the same set of dynamic critical exponents [2].

While the conventional pure and binary fluid have been extensively investigated both by theory and experiments (see, e.g., [2–6] for reviews), the critical dynamics of an *isothermal* compressible, single-component fluid seems not to have received much attention so far. Two-dimensional isothermal fluids are often used as simple models for monolayer films that are confined to liquid interfaces [7–9]. Indeed, many of these films are also known to undergo liquid-vapor-like phase transitions [10–12]. Recently, there has been growing interest in understanding the critical properties of these and related lipid bilayer systems [13–22], especially, since they constitute the building blocks that form the membranes of biological cells [23]. Since mono- and bilayers have critical temperatures of the order of the human body temperature, their critical dynamics might also have important consequences for physiology [21, 23–25]. Isothermal non-ideal fluid models have also been used to study phase-separation [26–32], capillary waves [33, 34] and supercooled liquids close to the glass transition [35–39]. All these works, however, did not address the critical dynamics of an isothermal fluid.

In this work, using a mode-coupling approach, it is demonstrated that the isothermal condition leads to decisively different dynamic critical properties than in the standard model H universality class. A scaling analysis of the leading self-energy contributions emerging from the nonlinear Langevin equations shows that the order-parameter dynamics effectively reduces to a time-dependent Ginzburg-Landau model for a non-conserved order parameter, known as *model A* [2]. The upper critical dimension, $d_c = 4$, is the same in statics and dynamics. The bulk viscosity diverges at the critical point with an exponent larger than in the mean-field limit, leading to overdamped sound modes at criticality. The shear viscosity, in contrast, remains finite, except for a possible weak divergence in two dimensions. The theoretical analysis is complemented by lattice Boltzmann simulations of the fluctuating hydrodynamics equations in two dimensions. We find that, even in this low dimensionality, the values of the critical exponents for the order parameter and bulk viscosity agree well with the analytical predictions that are obtained close to d_c based on pure model-A behavior.

In order to appreciate the difference of isothermal critical dynamics from that of a non-isothermal fluid, it is useful to recapitulate the basic results of the model H universality class. The original, incompressible model H consists of an advection-diffusion equation for the order parameter ϕ , which is coupled to a transverse velocity field \mathbf{u} [2, 6, 42, 50, 51],

$$\partial_t \phi = -\nabla \cdot (\phi \mathbf{u}) + \lambda \nabla^2 \frac{\delta}{\delta \phi} \mathcal{F} + \pi, \quad (1)$$

	isothermal		model H	
order parameter	mass density		entropy density (concentration)	
o.p. relaxation mechanism	sound waves		thermal diffusion (concentration diffusion)	
relevant nonlinearity for non-classical ¹ behavior	thermodynamic pressure		advection term	
sound speed	isothermal, $c_s^2 \sim \xi^{-\gamma/\nu}$		adiabatic, $c_s^2 \sim \xi^{-\alpha/\nu}$	
critical indices	2D	3D	2D	3D
order-parameter relaxation rate, $\Gamma \propto \xi^{-z}$	$2 - \eta + x$ 2.2 ± 0.1 2.08 ²		$d + y$ $1.98 \dots 2.15$ ⁴ 3.07 ⁵	
bulk viscosity, $\zeta_b \propto \xi^x$	$\sim 1.7\eta$ 0.45 ± 0.1 0.12 ²		$z - \alpha/\nu$ $1.98 \dots 2.15$ ⁴ 2.9 ⁶	
shear viscosity, $\zeta_s \propto \xi^y$	$z - d$ 0.2 ± 0.1 ³ finite		$-0.02 \dots 0.15$ ⁴ 0.07 ⁵	

TABLE I: Comparison of characteristic properties and critical indices of an isothermal compressible fluid and an energy-conserving pure fluid (or a binary fluid at the demixing point) described by model H. The cited numerical values are rounded, see the original works for more detailed predictions. Remarks: ¹“non-classical” refers to deviations from predictions of van-Hove theory, which assumes constant kinetic coefficients (see text). ²Theoretical predictions (averaged) based on model A [40, 41]. ³Prediction of the scaling theory. Present simulations, however, only reveal a finite critical contribution to the shear viscosity. See text for further discussion. ⁴Extrapolation of the ϵ -expansion results [2, 42] to 2D. ⁵see [43–47]. ⁶see [48]. Static critical exponents have Ising values [1, 49] and are identical for the isothermal and conventional (model H) fluid. ν is the correlation length exponent, $\gamma = (2 - \eta)\nu$ the susceptibility exponent, η the anomalous dimension exponent and α the specific heat exponent.

$$\rho_0 \partial_t \mathbf{u} = - \left(\phi \nabla \frac{\delta}{\delta \phi} \mathcal{F} \right)_{\perp} + \zeta_s \nabla^2 \mathbf{u} + \bar{\pi}_{\perp}, \quad (2)$$

where the label \perp indicates that the transverse projection should be taken, i.e., the projection orthogonal to the wavevector in Fourier space (cf. sec. II). In the above equations, ρ_0 is the mass density of the fluid, \mathcal{F} is a Ginzburg-Landau free energy functional, λ is a bare kinetic coefficient (thermal conductivity), ζ_s is the shear viscosity and π and $\bar{\pi}$ are appropriate noise sources. Importantly, in the case of a pure fluid at the liquid-vapor critical point, the relevant dynamical order parameter ϕ is the entropy density, whereas for a binary fluid at the demixing point, ϕ represents the concentration. The longitudinal part of the momentum density is neglected in the original model H, as the fluid is assumed to be incompressible, $\nabla \cdot \mathbf{u} = 0$. This is a valid approximation at criticality, since thermal conduction (or, correspondingly, concentration diffusion in a binary fluid) proceeds on a much longer timescale than the propagation of sound waves. The latter process is therefore irrelevant to the dynamics of the order parameter [50, 52]. In model H, the order-parameter relaxation rate is given in Fourier space by

$$\Gamma \sim \frac{\lambda k^2}{\chi(k)} \propto k^z, \quad (3)$$

with $\chi(k)$ being the susceptibility (isothermal compressibility) [2, 6]. This relation can be derived from eqs. (1) and (2) by linearizing and neglecting the advection term. Since $\chi(k) \propto k^{-2+\eta}$, the “classical” (van Hove [53]) theory predicts a dynamic critical exponent of $z = 4 - \eta$ for model H. The classical result, however, turns out to be violated in a real fluid, since the kinetic or transport coefficients are, due to the presence of reversible mode-couplings, affected by the critical order-parameter fluctuations as well [2, 54–56]. Specifically, in model H, the kinetic coefficient λ is renormalized by the nonlinear advective coupling between ϕ and \mathbf{u} , changing the dynamical exponent to $z = 4 - \eta - z_{\lambda} = d + y$, where z_{λ} and y are the exponents characterising the divergence of λ and the shear viscosity ζ_s , respectively [42–44, 51, 54, 57]. This value of z is also close to the predictions of early mode-coupling approaches, $z \simeq d$ [50, 58]. The effect of critical fluctuations on the shear viscosity, $\zeta_s \propto \xi^y$, is comparatively weak, leading only to a small exponent $y \simeq 0.07$ in 3D [42, 47, 54, 57], as confirmed by experiments [45, 46].

Critical fluctuations in a pure fluid have an effect on sound waves as well, which, however, is one-sided since the latter are decoupled from the order-parameter dynamics. Acoustic effects can be studied with an extended, compressible version of model H that includes the full set of equations for the mass, momentum and energy density [48, 59–67] (see also [68] and references therein). In an energy-conserving pure fluid, sound waves propagate with the *adiabatic* speed of sound [69–71],

$$c_{s,\text{ad}}^2 = \left. \frac{\partial p}{\partial \rho} \right|_S = \frac{c_p}{c_V} \frac{1}{\rho \chi}, \quad (4)$$

where p is the pressure and c_p , c_V are the specific heats at constant pressure and volume. These are related by $c_p = c_V + T\chi\beta_V^2/\rho$, where $\beta_V = (\partial p/\partial T)|_\rho$ is the thermal pressure coefficient (slope of the $p-T$ -curve). Since β_V is not critical, we have $c_p \sim \chi$ and hence the critical behavior of the speed of sound (at zero frequency) is given by [6, 48, 64, 68]

$$c_{s,\text{ad}}^2 \sim c_V^{-1} \propto \xi^{-\alpha/\nu}. \quad (5)$$

For comparison, in a binary fluid, the critical sound speed is governed by the constant-pressure specific heat, whose divergence is – due to a larger background contribution – much less pronounced than for the pure fluid. The critical sound damping is given by the bulk viscosity, which can be determined from a Green-Kubo relation involving the nonlinear pressure fluctuations [48, 59–61]. The extended model H predicts a strongly diverging bulk viscosity, $\zeta_b \propto \xi^x$ (at zero frequency), with $x = z - \alpha/\nu$ being $\simeq 2.9$ in 3D.

While theoretical and experimental investigations of critical dynamics in pure or binary fluids have a long history, simulations are scarce and have been performed only quite recently [72–77]. However, most of these studies are in 3D, and values of the dynamic critical exponents for model H in 2D seem so far not to have been obtained either by experiment or simulations (cf. [21, 78–83]). The values given in Tab. I for model H therefore correspond to extrapolations of theoretical ϵ -expansion results [2, 42] to 2D (throughout this paper $\epsilon = 4 - d$). The shear-viscosity exponent y in Tab. I has been computed using the ϵ -expansion result for z_λ in conjunction with the relation $y = 4 - d - \eta - z_\lambda$, giving the lower bound, as well as the direct ϵ -expansion result for y , giving the upper bound. Since the $O(\epsilon^2)$ -term in the ϵ -expansion of z_λ is quite small relative to the leading term, one might suspect that the extrapolated value will not be grossly unrealistic. Of course, one has to keep in mind that, even in the non-critical case, transport coefficients in a two-dimensional fluid acquire logarithmic divergences in the long-time or -wavelength limit [84–87], which might interfere with the critical divergences.

From relation (4) we see that a description in terms of the isothermal speed of sound,

$$c_{s,\text{iso}}^2 = \left. \frac{\partial p}{\partial \rho} \right|_T = \frac{1}{\rho \chi}, \quad (6)$$

would become applicable if the specific heat ratio c_p/c_V would be close to one. Dynamically, adiabatic conditions are achieved if the thermal relaxation rate [eq. (3)] is much smaller than the characteristic frequency of a sound wave, i.e.,

$$\Gamma \ll c_s k. \quad (7)$$

Since $c_{s,\text{ad}} k \propto \xi^{-\alpha/\nu-1}$ at $k \sim \xi^{-1}$, above relation is clearly fulfilled in a ordinary fluid close to the critical point. Relation (7) provides a posteriori also a justification for neglecting the “faster” acoustic processes in usual model H calculations. Far from criticality, violations of condition (7) can occur at finite wavenumbers in the hydrodynamic regime. Isothermal conditions can thus be only achieved by coupling to fluid to some kind of heat bath, so that temperature fluctuations are removed at a sufficiently fast rate. On the other hand, the friction between fluid and substrate should be sufficiently small, in order not to break momentum conservation and violate the characteristic sound mode behavior of the compressible fluid in the relevant wavenumber regime [88]. After these introductory remarks on the critical dynamics of ordinary non-ideal fluids, we now turn to the analysis of the isothermal non-ideal fluid.

II. THEORY

An isothermal compressible fluid is governed by a continuity equation for the density ρ and a conservation equation for the momentum $\mathbf{j} \equiv \rho \mathbf{u}$ [6, 26, 33, 69],

$$\partial_t \rho = -\nabla \cdot \mathbf{j}, \quad (8)$$

$$\partial_t \mathbf{j} = -\rho \nabla \frac{\delta \mathcal{F}}{\delta \rho} + \zeta_s \nabla^2 \frac{\mathbf{j}}{\rho} + (\zeta_b + \zeta_s[1 - 2/d]) \nabla \nabla \cdot \frac{\mathbf{j}}{\rho} + \nabla \cdot \mathbf{R}. \quad (9)$$

Here, ζ_s and ζ_b are the bare shear and bulk viscosity and \mathbf{R} is a random stress tensor with correlations [69, 89]

$$\langle R_{\alpha\beta}(\mathbf{r}, t) R_{\gamma\delta}(\mathbf{r}', t') \rangle = 2k_B T \left[\zeta_s \left(\delta_{\alpha\gamma} \delta_{\beta\delta} + \delta_{\alpha\delta} \delta_{\beta\gamma} - \frac{2}{d} \delta_{\alpha\beta} \delta_{\gamma\delta} \right) + \zeta_b \delta_{\alpha\beta} \delta_{\gamma\delta} \right] \delta(\mathbf{r} - \mathbf{r}') \delta(t - t'), \quad (10)$$

imparting Gaussian thermal noise on the fluid. The static probability distribution of the density fluctuations are governed by the Ginzburg-Landau free energy functional

$$\mathcal{F} = \int dV \left[\frac{1}{2} \kappa (\nabla \phi)^2 + f_0(\phi) \right], \quad (11)$$

where κ is a constant and

$$\phi \equiv (\rho - \rho_0)/\rho_0 \quad (12)$$

is the order parameter. ρ_0 is a constant background density. The Landau free energy density f_0 is taken to be a quartic polynomial in ϕ ,

$$f_0(\phi) = \frac{1}{2} r \phi^2 + \frac{1}{4} u \phi^4. \quad (13)$$

The “streaming term” involving \mathcal{F} in eq. (9) can be written as divergence of a pressure tensor \mathbf{P} [33, 90–94],

$$\rho \nabla \frac{\delta \mathcal{F}}{\delta \rho} = \nabla \cdot \mathbf{P} = \nabla p_0 - \frac{\kappa}{\rho_0^2} \rho \nabla \nabla^2 \rho \quad (14)$$

where

$$P_{\alpha\beta} = \left(p_0 - \kappa \rho \nabla^2 \rho - \frac{\kappa}{2} |\nabla \rho|^2 \right) \delta_{\alpha\beta} + \kappa (\partial_\alpha \rho) (\partial_\beta \rho), \quad (15)$$

and the scalar pressure p_0 is given by

$$p_0 = \rho \partial_\rho f_0 - f_0 = r \phi + \frac{1}{2} r \phi^2 + u \phi^3 + \frac{3}{4} u \phi^4. \quad (16)$$

An essential complication in the analysis of the compressible Navier-Stokes equations is the presence of the non-linearity \mathbf{j}/ρ in the viscous stress [36, 39, 95]. Here, we treat this term perturbatively by expanding $1/\rho$ around the background density ρ_0 , i.e. $1/\rho = 1/\rho_0 - (1/\rho_0^2) \delta \rho + \dots$ [96, 97]. We find that this term is irrelevant for the critical behavior of the fluid above two dimensions. Furthermore, in the above Navier-Stokes equations, the convection term $\nabla(\rho \mathbf{u} \mathbf{u})$ has been neglected, since the effect of this term is well known and not specifically related to critical phenomena [84–87]. Above two dimensions, the convective nonlinearity gives a finite contribution to the renormalization of the shear and bulk viscosity, while logarithmic divergences appear in 2D in the limit of large time- or length-scales. In principle, these effects require careful treatment, also regarding a possible interplay with critical fluctuations. This, however, is out of the scope of the present work, and in the subsequent analysis, it is therefore assumed that these effects are either already included in the bare viscosities or can be considered separately from critical fluctuations.

To proceed, eqs. (8) and (9) are written in Fourier space,

$$\omega \delta \rho = \mathbf{k} \cdot \mathbf{j}, \quad (17)$$

$$-i \omega \mathbf{j} = -i \mathbf{k} c_s^2(\mathbf{k}) \delta \rho - i \mathbf{k} p_{\text{nl}} - i \mathbf{N} - \nu_s k^2 [\mathbf{j} + \mathbf{Y}] - (\nu_b + \nu_s[1 - 2/d]) \mathbf{k} \mathbf{k} \cdot [\mathbf{j} + \mathbf{Y}] + i \mathbf{k} \cdot \mathbf{R} + i \mathbf{k} \cdot \mathbf{h}, \quad (18)$$

where $\nu_s = \zeta_s/\rho_0$ and $\nu_b = \zeta_b/\rho_0$ are the kinematic shear and bulk viscosities. The generalized isothermal speed of sound [127]

$$c_s^2(\mathbf{k}) = c_s^2 + \kappa \rho_0 k^2 = r/\rho_0 + \kappa \rho_0 k^2, \quad (19)$$

contains the linear part of the thermodynamic pressure, while p_{nl} and \mathbf{N} are the Fourier-transforms of the remaining nonlinear parts:

$$p_{\text{nl}}(\mathbf{k}, \omega) = \frac{1}{2} r \int_{\tilde{q}} \phi(\tilde{k} - \tilde{q}) \phi(\tilde{q}) + u \int_{\tilde{q}, \tilde{q}'} \phi(\tilde{k} - \tilde{q} - \tilde{q}') \phi(\tilde{q}) \phi(\tilde{q}') + \frac{3}{4} u \int_{\tilde{q}, \tilde{q}', \tilde{q}''} \phi(\tilde{k} - \tilde{q} - \tilde{q}' - \tilde{q}'') \phi(\tilde{q}) \phi(\tilde{q}') \phi(\tilde{q}''), \quad (20)$$

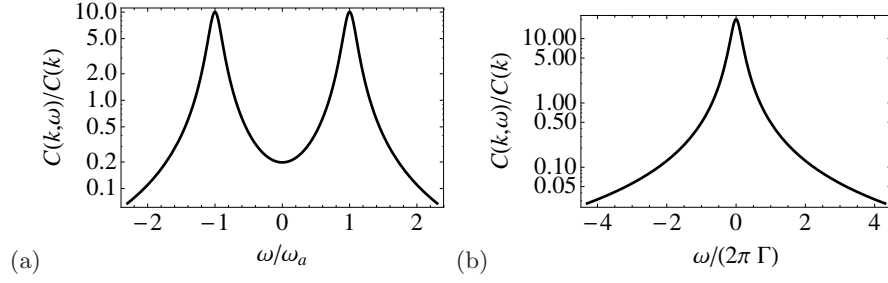


FIG. 1: Typical shape of the dynamic structure factor $C(k, \omega)$ in an isothermal fluid in the weak-damping (a) and strong-damping (b) regime.

$$\mathbf{N}(\mathbf{k}, \omega) = \kappa \int_{\tilde{q}} \phi(\tilde{k} - \tilde{q}) \mathbf{q} q^2 \phi(\tilde{q}), \quad (21)$$

Here, the shorthand notation $\tilde{k} \equiv (\mathbf{k}, \omega)$, $\tilde{q} \equiv (\mathbf{q}, \sigma)$, etc. and $\int_{\tilde{q}} \equiv \int \frac{d\mathbf{q}}{(2\pi)^d} \frac{d\sigma}{(2\pi)}$ is introduced. The quantity

$$\mathbf{Y}(\mathbf{k}, \omega) = \int_{\tilde{q}} \mathbf{j}(\tilde{q}) \phi(\tilde{k} - \tilde{q}) \quad (22)$$

represents the leading correction term of the expansion of \mathbf{j}/ρ around \mathbf{j}/ρ_0 .

The nonlinear Navier-Stokes equations (17) and (18) can be split into longitudinal and transverse parts with respect to the wavevector \mathbf{k} . The corresponding longitudinal ('l') and transverse ('t') projections of a vectorial quantity $\mathbf{v} = v_l \hat{\mathbf{k}} + \mathbf{v}_t$ are defined as $v_l = \hat{\mathbf{k}} \cdot \mathbf{v}$ and $\mathbf{v}_t = \mathcal{T}_{\mathbf{k}} \mathbf{v}$, where $\hat{\mathbf{k}} \equiv \mathbf{k}/k$ and $\mathcal{T}_{\mathbf{k}} \equiv (\mathbb{I} - \hat{\mathbf{k}} \hat{\mathbf{k}})$. Analogously, for a tensorial quantity \mathbf{R} , we have $\hat{\mathbf{k}} \cdot \mathbf{R} = R_l \hat{\mathbf{k}} + \mathbf{R}_t$, with $R_l \equiv \hat{\mathbf{k}} \cdot \mathbf{R} \cdot \hat{\mathbf{k}}$, and $\mathbf{R}_t \equiv \hat{\mathbf{k}} \cdot \mathbf{R} \cdot \mathcal{T}_{\mathbf{k}}$. We thus arrive at

$$\omega \delta \rho = k j_l, \quad (23)$$

$$\omega j_l = k c_s^2(\mathbf{k}) \delta \rho + k p_{nl} + N_l - i \nu_l k^2 (j_l + Y_l) - k R_l - k h_l, \quad (24)$$

$$\omega \mathbf{j}_t = \mathbf{N}_t - i \nu_t k^2 (\mathbf{j}_t + \mathbf{Y}_t) - k \mathbf{R}_t - k \mathbf{h}_t, \quad (25)$$

where $\nu_l = \nu_b + \nu_s(2 - 2/d)$ denotes the longitudinal and $\nu_t = \nu_s$ the transverse viscosity. The longitudinal and transverse parts of the random stress tensor are correlated as $\langle |R_l(\mathbf{k}, \omega)|^2 \rangle = 2\rho_0 \nu_l k_B T$ and $\langle |R_{t,\alpha}(\mathbf{k}, \omega)|^2 \rangle = 2\rho_0 \nu_t k_B T$. Combining eqs. (23) and (24), the longitudinal current j_l can be eliminated completely, leaving only eq. (25) for the transverse current and a single, nonlinear sound-wave equation for the order parameter (setting henceforth $\rho_0 = 1$):

$$-\omega^2 \phi + k^2 c_s^2(\mathbf{k}) \phi - i \nu_l \omega k^2 \phi = -k^2 p_{nl} - k N_l + i \nu_l k^3 Y_l + k^2 R_l + k^2 h_l. \quad (26)$$

Obviously, the term \mathbf{Y} , which can be written as

$$\mathbf{Y} = \int_{\tilde{q}} \left[\phi(\tilde{q}) \frac{\sigma}{q} \hat{\mathbf{q}} + \mathbf{j}_t(\tilde{q}) \right] \phi(\tilde{k} - \tilde{q}), \quad (27)$$

provides a bi-directional coupling between the order parameter and the transverse current. Additionally, the transverse current is affected by the order-parameter fluctuations through the term \mathbf{N}_t . Note that, due to the way the free energy functional enters the Navier-Stokes equations, there appear to be more nonlinearities in eq. (26) than the corresponding static critical theory or in nonlinear sound-wave equations studied in isotropic elastic phase transitions [98, 99]. In the latter, the restoring force is given by a term $\sim \delta \mathcal{F} / \delta \rho$ rather than by a pressure gradient.

A. Linear hydrodynamics

At this point it is useful to collect some basic results of the linear model. Neglecting the nonlinear terms in eq. (26), the *bare* response- and correlation function (labeled by an index 0) for the order parameter are given by

$$G_0(\mathbf{k}, \omega) \equiv \frac{\delta \langle \phi(\mathbf{k}, \omega) \rangle}{\delta h_l(\mathbf{k}, \omega)} = \frac{k^2}{-\omega^2 + k^2 c_s^2(\mathbf{k}) - i \nu_l \omega k^2}, \quad (28)$$

$$C_0(\mathbf{k}, \omega) \equiv \langle \phi(\mathbf{k}, \omega) \phi(\mathbf{k}', \omega') \rangle / (2\pi)^{d+1} \delta(\mathbf{k} + \mathbf{k}') \delta(\omega + \omega') = \frac{2\nu_l k_B T k^4}{[\omega^2 - k^2 c_s^2(\mathbf{k})]^2 + (\omega \nu_l k^2)^2}. \quad (29)$$

The response and correlation functions are related by a fluctuation-dissipation theorem,

$$C_0(\mathbf{k}, \omega) = \frac{2k_B T}{\omega} \text{Im} G_0(\mathbf{k}, \omega), \quad (30)$$

which, in the zero-frequency limit, becomes the fluctuation-response relation

$$C_0(\mathbf{k}) = k_B T G_0(\mathbf{k}, \omega = 0), \quad (31)$$

where $C(\mathbf{k})$ is the static structure factor,

$$C_0(\mathbf{k}) = \int \frac{d\omega}{2\pi} C_0(\mathbf{k}, \omega) = \frac{k_B T}{c_s^2(\mathbf{k})}. \quad (32)$$

In the linear case, eq. (26) represents a damped harmonic oscillator driven by random noise [49]. The dispersion relation of the associated sound waves is given by

$$\omega = \pm [c_s^2(k)k^2 - \nu_l^2 k^4/4]^{1/2} - i\nu_l k^2/2. \quad (33)$$

In the weakly damped case, where $c_s^2(k) > \nu_l^2 k^2$, sound waves are oscillating with frequencies $\omega_a = \pm k [c_s^2(k) - \nu_l^2 k^2/4]^{1/2} \approx c_s(k)k$ and are exponentially damped with a rate of $\nu_l k^2/2$. In the opposite, overdamped case, the solution (33) becomes purely imaginary and sound waves decay, in the limit of long times, with a rate of

$$\Gamma(\mathbf{k}) = \frac{c_{sR}^2(\mathbf{k})}{\nu_{lR}}. \quad (34)$$

At short times, there is another decay regime with a rate $\sim \nu_l k^2$, which, however, is negligible if $c_s^2 \gg \nu_l^2 k^2$. The response and correlation functions in the overdamped, long-time limit can be obtained by neglecting the “inertial” term ω^2 in eqs. (28) and (29), yielding

$$G_0(\mathbf{k}, \omega) = \frac{1}{-i\nu_{lR}(\mathbf{k})\omega + c_{sR}^2(\mathbf{k})}, \quad (35)$$

$$C_0(\mathbf{k}, \omega) = \frac{1}{\nu_{lR}(\mathbf{k})} \frac{2k_B T}{\omega^2 + \Gamma^2(\mathbf{k})}. \quad (36)$$

In the time-domain, this corresponds to a pure exponential decay:

$$G_0(\mathbf{k}, t) = \frac{1}{\nu_{lR}(\mathbf{k})} \exp[-\Gamma(\mathbf{k})t] \theta(t), \quad (37)$$

$$C_0(\mathbf{k}, t) = C(\mathbf{k}) \exp[-\Gamma(\mathbf{k})|t|]. \quad (38)$$

Similarly, for the transverse current, we obtain from eq. (25) the bare response and correlation functions

$$G_{t,0}(\mathbf{k}, \omega) = \frac{k}{\omega + i\nu_t k^2}, \quad (39)$$

$$C_{t,0}(\mathbf{k}, \omega) = \frac{2\nu_t k_B T k^2}{\omega^2 + (\nu_t k^2)^2}, \quad (40)$$

where $\langle j_{t,\alpha}(\mathbf{k}, \omega) j_{t,\beta}(\mathbf{k}', \omega') \rangle = C_{t,0}(\mathbf{k}, \omega) (2\pi)^{d+1} \delta(\mathbf{k} + \mathbf{k}') \delta(\omega + \omega') \delta_{\alpha\beta}$. The static correlations of the transverse current are independent of the wavenumber,

$$C_t(\mathbf{k}) = k_B T. \quad (41)$$

The linear hydrodynamics expressions (28) and (29) can be cast into standard dynamical scaling forms [2, 49, 100],

$$G_0(\mathbf{k}, \omega) = \xi^{2-\eta} \mathcal{G}(k\xi, \omega\xi^z), \quad C_0(\mathbf{k}, \omega) = \xi^{2-\eta+z} \mathcal{C}(k\xi, \omega\xi^z), \quad (42)$$

with \mathcal{G} and \mathcal{C} being scaling functions, $\eta = 0$ and a dynamic scaling exponent of $z = 2$. This value of z can also be inferred from the damping rate in the overdamped case, eq. (34). Analogously, for the transverse current, eqs. (39) and (40), we have

$$G_{t,0}(\mathbf{k}, \omega) = \xi^{z_t-1} \mathcal{G}_t(k\xi, \omega\xi^{z_t}), \quad C_{t,0}(\mathbf{k}, \omega) = \xi^{z_t} \mathcal{C}_t(k\xi, \omega\xi^{z_t}), \quad (43)$$

with a dynamic exponent of $z_t = 2$.

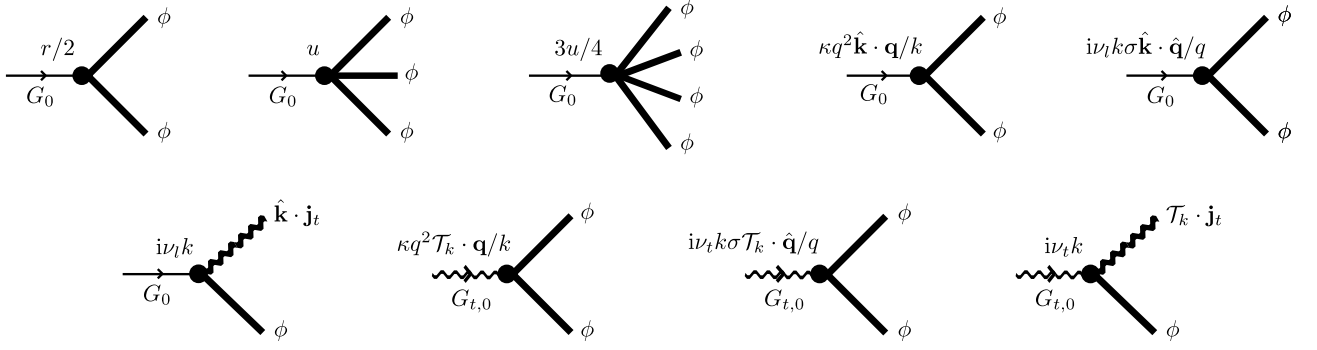


FIG. 2: Fundamental vertices of the model arising from eqs. (20), (21) and (22). Here, \mathbf{k} is an external wavevector, while \mathbf{q} and σ denote an internal wavevector and frequency. A filled circle represents a coupling constant and an integration over internal wavevectors and frequencies respecting space- and time-translational invariance.

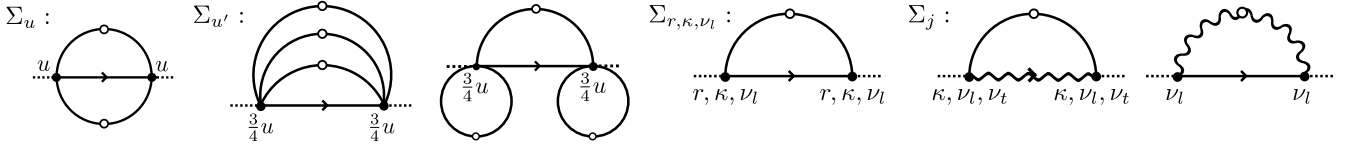


FIG. 3: Leading frequency-dependent diagrams contributing to the self-energy of the order parameter, $\Sigma(\mathbf{k}, \omega)$. A solid (wavy) line with an arrow represents G_0 ($G_{t,0}$) and a solid line with an open circle C_0 ($C_{t,0}$). Dashed lines indicate amputated external “legs” for clarity.

B. Critical order-parameter dynamics

The critical dynamics of the order parameter, governed by eq. (26), is discussed here within a mode-coupling approach [6, 50, 54, 56, 101, 102]. To this end we shall construct a perturbative solution of the nonlinear order-parameter equation using the response function formalism [55, 100, 103, 104] and identify the leading contributions via a scaling analysis. With the help of the bare response function G_0 , eq. (26) can be rearranged as

$$\phi = \phi_0 - G_0 p_{\text{nl}} - G_0 N_l / k + i \nu_l k G_0 Y_l + G_0 h_l, \quad (44)$$

with $\phi_0 = G_0 R_l$ being the zeroth-order solution. Due to the coupling between the order parameter and the transverse current, we also need to consider eq. (25), which can be written as

$$\mathbf{j}_t = -\mathbf{j}_{t,0} + G_{t,0} \mathbf{N}_t / k - i \nu_t k \mathbf{Y}_t - G_{t,0} \mathbf{h}_t, \quad (45)$$

with $\mathbf{j}_{t,0} = G_{t,0} \mathbf{R}_t$.

The nonlinearities on the right hand side of eqs. (44) and (45) can be translated into a diagrammatic representation as given by Fig. 2. There, a solid (wavy) line with an arrow represents G_0 ($G_{t,0}$), a thick solid line represents the order parameter ϕ , a filled circle stands for a coupling constant and an integration over internal wavevectors and frequencies respecting space- and time-translational invariance. The vertices involving the couplings r , κ , ν_l and ν_t have no counterparts in the static theory or in standard Ginzburg-Landau models [2] and are specific to the compressible fluid. They arise already from the Gaussian part of the free energy functional and are known to be important in the case of a supercooled liquid [36, 39].

A solution of eq. (44) for ϕ can be iteratively constructed, following standard rules [50, 55, 100, 103], and leads to a Dyson relation for the full response function $G \equiv \delta\langle\phi\rangle/\delta h_l$:

$$G(\mathbf{k}, \omega) = \frac{1}{G_0^{-1}(\mathbf{k}, \omega) - \Sigma(\mathbf{k}, \omega)} = \frac{k^2}{-\omega^2 + k^2 c_s^2(\mathbf{k}) - i \nu_l \omega k^2 - k^2 \Sigma(\mathbf{k}, \omega)}. \quad (46)$$

Here, Σ is a self-energy, which encapsulates the effect of the nonlinear interactions between the order-parameter fluctuations. These can be understood to lead to a renormalization of the transport coefficients of the fluid of the form

$$c_{sR}^2(\mathbf{k}) = c_s^2(\mathbf{k}) - \text{Re}\Sigma(\mathbf{k}, 0), \quad (47)$$

$$\nu_{lR}(\mathbf{k}) = \nu_l + \Pi(\mathbf{k}, \omega \rightarrow 0), \quad (48)$$

where $\Pi(\mathbf{k}, \omega) \equiv \partial \text{Im} \Sigma(\mathbf{k}, \omega) / \partial \omega$. We shall focus here only on the small-frequency limit and neglect any frequency-dependence of c_{sR} and ν_{lR} . Thus, we assume that the response function keeps the same principle form as in linear hydrodynamics, but with appropriately renormalized transport coefficients. Also, a possible renormalization of the background density is neglected here.

The nonlinearities in the model give rise to a large number of diagrams contributing to the static and dynamic (i.e., frequency-independent and -dependent) parts of the self-energy. The dominant contribution can in principle be determined through a straightforward scaling analysis (see, e.g., [54, 102]), making use of the dynamic scaling forms of the response and correlation functions stated above. Regarding the static parts, we can just invoke the fact that the nonlinear Langevin equations of the model preserve the equilibrium probability distribution of the Ginzburg-Landau free-energy functional [6, 89]. Thus, in the hydrodynamic limit, the renormalization of the isothermal speed of sound must be consistent with the static theory, implying that, $c_s^2 = 1/\rho\chi \propto \xi^{-\gamma/\nu}$, where χ is the isothermal compressibility, ξ the correlation length and γ and ν are the usual static critical exponents [note $\gamma = (2 - \eta)\nu$] [1, 3, 6] [128]. The upper critical dimension for statics is 4. In contrast, in a conventional fluid (model H), sound waves propagate with the adiabatic speed of sound, which vanishes much more weakly at the critical point, $c_s^2 \propto \xi^{-\alpha/\nu}$, with α being the specific heat exponent [1, 6, 48, 59, 64].

Turning to the dynamics, the leading irreducible, frequency-dependent diagrams contributing to Σ are shown in Fig. 3. For a given diagram $\Sigma_{(i)}$, we have $\Pi_{(i)} \sim \Sigma_{(i)}\xi^z$ as far as the scaling behavior is concerned. We do not consider here an expansion in the number of loops, but rather focus only on the leading diagrams arising from each vertex. The analytic expressions of the individual diagrams are given by

$$\Sigma_u(\mathbf{k}, \omega) = 18u^2 \int_{\tilde{q}, \tilde{q}'} G_0(\tilde{k} - \tilde{q} - \tilde{q}') C_0(\tilde{q}) C_0(\tilde{q}'), \quad (49)$$

$$\Sigma_{u'}(\mathbf{k}, \omega) = 54u^2 \int_{\tilde{q}, \tilde{q}', \tilde{q}''} G_0(\tilde{k} - \tilde{q} - \tilde{q}' - \tilde{q}'') C_0(\tilde{q}) C_0(\tilde{q}') C_0(\tilde{q}'') \quad (50)$$

$$+ 81u^2 \int_{\tilde{q}} G_0(\tilde{k} - \tilde{q}) C_0(\tilde{q}) \left[\int_{\tilde{q}} C_0(\tilde{q}) \right]^2, \quad (51)$$

$$\Sigma_r(\mathbf{k}, \omega) = r^2 \int_{\tilde{q}} G_0(\tilde{k} - \tilde{q}) C_0(\tilde{q}), \quad (52)$$

$$\Sigma_\kappa(\mathbf{k}, \omega) = \kappa^2 \int_{\tilde{q}} G_0(\tilde{k} - \tilde{q}) C_0(\tilde{q}) [(\mathbf{k} \cdot \mathbf{q})^2 + O(k^4)], \quad (53)$$

$$\Sigma_{\nu_l}(\mathbf{k}, \omega) = -\nu_l^2 \int_{\tilde{q}} G_0(\tilde{k} - \tilde{q}) C_0(\tilde{q}) [\omega \sigma(\hat{\mathbf{k}} \cdot \hat{\mathbf{q}})^2 + O(\omega^2)], \quad (54)$$

$$\Sigma_j(\mathbf{k}, \omega) = \nu_l \nu_t \int_{\tilde{q}} G_{t,0}(\tilde{q}) C_0(\tilde{k} - \tilde{q}) [\omega q (\hat{\mathbf{k}} \cdot \boldsymbol{\tau}_{\mathbf{q}} \cdot \hat{\mathbf{k}}) + O(\omega k)] \quad (55)$$

$$- \nu_l^2 \int_{\tilde{q}} G_0(\tilde{q}) C_{t,0}(\tilde{k} - \tilde{q}) [\mathbf{k} \cdot \mathbf{q} + O(k^2)] + \dots \quad (56)$$

In eqs. (53) to (56), only the principle form of the kernels is indicated, which is sufficient to derive scaling properties. Also, expressions for the remaining one-loop diagrams of Fig. 3 that involve two different couplings or a transverse current response/correlation function are not stated explicitly but can be easily obtained. In fact, it will not be necessary to compute them explicitly, since all vertices involving r , κ , ν_l or ν_t scale in the same way, up to differences of $O(\eta)$. To see this, note that j_t scales like $\phi\xi^{-1}$, as can be inferred from the form of the corresponding correlation functions [eqs. (42), (43)]. Some of the additional diagrams at two-loop order are briefly discussed in appendix A; they will give rise to subdominant contributions and can thus be safely neglected.

First of all, we consider the mean-field approximation, where the values of the dynamic scaling exponents are given by $z = z_t = 2$. Taking into account the strong temperature-dependence of the Landau parameter, $r \sim 1/\chi \sim \xi^{-2}$, we find, in the limit $k \rightarrow \xi^{-1}$, $\omega \rightarrow \xi^{-z}$:

$$\Pi_u \propto \xi^{8-2d}, \quad \Pi_{u'} \propto \xi^{10-3d}, \quad \Pi_{r,\kappa,\nu_l,j} \propto \xi^{2-d}. \quad (57)$$

The identical scaling of all one-loop diagrams of Fig. 3 is a consequence of the identical scaling behavior of the two-point vertices in the model. We can also obtain scaling predictions beyond the mean-field case by making use of our knowledge of the proper critical behavior of the static couplings, κ , r and u . These are renormalized by fluctuations

as $r_R \sim \xi^{-2+\eta}$, $\kappa_R \sim \xi^\eta$, $u_R \sim \xi^{d-4+2\eta}$ [6, 100], implying that

$$\Pi_u \propto \xi^{z-2+\eta}, \quad \Pi_{u',r,\kappa,\nu_l} \propto \xi^{z-d}. \quad (58)$$

The remaining contributions due to Π_j all scale $\propto \xi^{z-d \pm O(\eta)}$, or $\xi^{z-d \pm O(\eta)}$, respectively, up to differences in the exponent of $O(\eta)$ accounting for possible divergences of ν_l or ν_t . Thus, all diagrams except Π_u are irrelevant for $d > 2$, provided that z and z_t are still close to 2, which will indeed be the case. Note that the contributions from the $u\phi^4$ -vertex, which were found to diverge below a critical dimension of $d = 10/3$ in the mean-field limit, now remain finite at least down to three dimensions, owing to the renormalization of u . We also see that the \mathbf{j}/ρ -nonlinearity in eq. (9), responsible for the coupling between longitudinal and transverse current, is not relevant for $d > 2$ and it is safe to approximate ρ by ρ_0 , as far as asymptotic critical properties are concerned.

From the dominance of Σ_u , which arises from the ϕ^3 -vertex of p_{nl} , we conclude that the *upper critical dimension* of the present isothermal non-ideal fluid model is $d_c = 4$ *both* in statics and dynamics. The present analysis also reveals that the relevant nonlinearities responsible for the deviations from the classical (van Hove) predictions are different for the isothermal fluid and model H: in the latter case, the deviation is caused by the reversible advection term [see eq. (1)], whereas in the isothermal fluid, it is caused by the dissipative ϕ^4 -nonlinearity of the Ginzburg-Landau free energy functional. Hence, in the isothermal fluid, all dynamic critical effects are induced purely by thermodynamic quantities.

The scaling result for Π_u of eq. (58) is not sufficient to determine the precise value of z . This can be done via a renormalization group (RG) calculation slightly below four dimensions. To this end, the wavenumber integrations in Π_u of eq. (49) are performed incrementally in a shell $\Lambda_0 e^{-s} < q, q' < \Lambda_0$, where Λ_0 is a cutoff and s denotes the RG flow parameter. The contribution linear in s , which we shall write as $A(\nu_l)\nu_l$, has been calculated in [98], with the essential result that $A(\nu_l \rightarrow \infty) = 6 \ln(4/3)\eta$ and $A(\nu_l) > A(\infty)$ for any finite ν_l . These estimates have been obtained at $O(\epsilon^2)$ in an ϵ -expansion. The RG equation for the longitudinal viscosity then reads

$$\partial_s \nu_l(s) = A(\nu_l)\nu_l(s), \quad (59)$$

from which one concludes that, for any positive bare $\nu_l(0)$, $\nu_l(s)$ will grow along the RG flow and asymptotically scale as $e^{A(\infty)s}$. Thus, in the hydrodynamic limit, which is reached for $e^s \sim \Lambda_0 \xi$ [6, 105], the renormalized longitudinal viscosity behaves as

$$\nu_{lR} \propto \nu_l \xi^x, \quad (60)$$

with a critical index

$$x = 6 \ln(4/3)\eta \simeq 1.7\eta. \quad (61)$$

In the critical regime ($k \gg \xi^{-1}$), we have accordingly, $\nu_{lR} \propto \nu_l k^{-x}$. With this result, we can show that sound waves must be *overdamped* in the critical isothermal fluid: using the fact that $c_{sR}^2 \propto \xi^{-2+\eta}$, the linear hydrodynamical condition for strong damping, $c_{sR}(k) \ll k\nu_{lR}$, becomes $\xi^{-1+\eta/2}/k + \text{const.} \times k^{-\eta/2} \ll \xi^x$. Thus, for wavenumbers of order $k \sim \xi^{-1}$, we have $\xi^\eta \ll \xi^{2x}$, which is always fulfilled in the asymptotic critical regime since $2x > \eta$. Of course, we could also have kept, for d close to d_c , only the dominant $u\phi^3$ -nonlinearity in eq. (26) and thereby recover the type of sound-wave equation studied in the context of isotropic elastic phase transitions [98]. The associated RG analysis in [98] then leads to the same predictions as above.

Concluding, in the critical regime, eq. (26) reduces in the long-time limit to *model A* in the classification of [2, 106–108], that is, a time-dependent Ginzburg-Landau model for a non-conserved order parameter,

$$-i\omega\delta\rho = \frac{1}{\nu_l} \frac{\delta\mathcal{F}}{\delta\rho} + \mathcal{R} + h_l, \quad (62)$$

where $\mathcal{R} \equiv R_l/\nu_l$ is a noise source of variance $\sim 1/\nu_l$ [129]. Since overdamped sound waves relax with a rate

$$\Gamma = \frac{c_{sR}^2}{\nu_{lR}}, \quad (63)$$

the dynamic critical index z , defined via $\Gamma \sim \xi^z$, of the fully nonlinear fluid model follows as

$$z = 2 - \eta + x. \quad (64)$$

In contrast, in the linear hydrodynamic (mean-field) case, we have $z = 2$ and $x = 0$. If we assume that the pure model-A behavior of the critical isothermal fluid persists also in low dimensions, we expect, in the interesting two-dimensional case, a value of

$$z \simeq 2.08 \dots 2.17 \quad (2D), \quad (65)$$

based on recent theoretical calculations and Monte Carlo simulations of model A [40, 41, 109]. In the wider literature, varying estimates for z , ranging between 2.0 to 2.3, have been reported [110, 111]. Above value for z translates to $x \simeq 0.4$ and agrees surprisingly well with the $O(\epsilon^2)$ -renormalization-group prediction of eq. (61) in 2D. For comparison, for a conventional fluid (model H), $z \simeq d$ and $x = z - \alpha/\nu$ [2, 6, 48].

Returning to the scaling estimates of eq. (58), a value of $z > 2$ would imply the weak divergence of various diagrams in 2D, which could provide corrections to the critical exponents. To address this issue, explicit calculations of the corresponding contributions will be required. Our simulations (see sec. III), however, yield a value of $z \approx 2.2 \pm 0.1$, suggesting that possible corrections to the model-A behavior are small at least.

C. Critical shear viscosity

The shear viscosity is discussed in the following based on a Green-Kubo approach. We consider the x -component of the nonlinear NSE (9) and choose the wavevector to lie along the y -direction, i.e. $\mathbf{k} = (0, k)$ in 2D. Applying the approximation $\mathbf{j}/\rho \simeq \mathbf{j}/\rho_0 + (\mathbf{j}/\rho_0^2)\delta\rho$ to the viscous stress tensor, whose xy -component becomes

$$S_{xy} = \nu_s[\partial_x(j_y + j_y\phi) + \partial_y(j_x + j_x\phi)] \quad (66)$$

the equation for the transverse current can be written as

$$\partial_t j_x = -\nu_s k^2 j_x - ikP_{xy}(\mathbf{k}) + ikS_{xy}^{\text{nl}}(\mathbf{k}) + ikR_{xy}, \quad (67)$$

where $P_{xy}(\mathbf{k}, t) = -\kappa \int_{\mathbf{q}} q_x q_y \phi(\mathbf{q})\phi(\mathbf{k} - \mathbf{q})$ is the Fourier-transform of the off-diagonal term of the thermodynamic pressure tensor [eq. (15)], while $S_{xy}^{\text{nl}}(\mathbf{k}, t) = i\nu_s k \int_{\mathbf{q}} j_x(\mathbf{q}, t)\phi(\mathbf{k} - \mathbf{q}, t)$ contains the nonlinear terms of S_{xy} [eq. (66)] involving the order parameter.

The fluctuation contribution to the shear viscosity, $\nu_{s,\text{crit}}$, can now be inferred by invoking a Green-Kubo relation [6, 47, 112]. For the contribution from the thermodynamic pressure tensor we find

$$\nu_{s,\text{crit}} = \frac{1}{Vk_B T} \lim_{k \rightarrow 0} \int_0^\infty dt \langle P_{xy}(\mathbf{k}, t) P_{xy}(-\mathbf{k}, 0) \rangle \simeq \frac{\kappa^2}{k_B T} \int_{\mathbf{q}} q_x^2 q_y^2 \frac{C^2(\mathbf{q})}{\Gamma(\mathbf{q})} \propto \xi^{z-d}, \quad (68)$$

where, as usual, the four-point correlation has been decoupled into products of two-point correlation functions. For the contribution due to the nonlinear part of the viscous stress tensor, S_{xy} , one writes $j_x(\mathbf{q}) = j_l(\mathbf{q})\hat{q}_x + \mathbf{j}_{t,x}(\mathbf{q})$ and uses the fact that the correlation function of the longitudinal current fulfills $C_l(\mathbf{q}, t) = \partial_t^2 C(\mathbf{q}, t)/q^2$. Also, j_l and \mathbf{j}_t are independent to leading order. This gives analogously

$$\nu'_{s,\text{crit}} = \frac{1}{Vk_B T} \lim_{k \rightarrow \xi^{-1}} \int_0^\infty dt \langle S_{xy}^{\text{nl}}(\mathbf{k}, t) S_{xy}^{\text{nl}}(-\mathbf{k}, 0) \rangle \propto \xi^{4-z-d-2\eta} + \xi^{z_t-\eta-d}, \quad (69)$$

where the external wavevector is taken at ξ^{-1} and, for the evaluation of the part involving the transverse current, it has been assumed that $z_t < z$. In the mean-field limit, all contributions scale $\propto \xi^{2-d}$ and thus are finite for $d > 2$, while a potential logarithmic divergence is indicated in 2D. If, in contrast, scaling exponents appropriate for the true critical point are taken (where $z \simeq 2.2$ and $\kappa_R \propto \xi^\eta$), the contribution to $\nu_{s,\text{crit}}$ of eq. (68) attains a weak power-law divergence in 2D, characterized by a critical exponent $y = z - 2$, implying that $z_t = 2 - y < 2$ in 2D. As a consequence, eq. (69) becomes now finite in all dimensions. In our simulations, however, where we evaluate the critical shear viscosity using eq. (68), we do not observe a divergence in 2D. This might be related to limitations of the simulation model and is discussed further in sec. III B 2. Note that the same calculation as in eq. (68) applies to model H as well. There, the shear viscosity diverges mildly in 3D, due to a value of $z \simeq 3.07$ that is slightly larger than 3 [2, 47]. In 2D, the uncertainty in the theoretical value for z (see Tab. I) and the lack of experimental or numerical studies permits no definite conclusion on a possible critical divergence of the shear viscosity in an ordinary fluid.

III. SIMULATIONS

The theoretical predictions are now compared to full fluctuating hydrodynamics simulations of a non-ideal fluid in 2D, using the Lattice Boltzmann (LB) model introduced in [113]. Results on the static critical behavior of the model, which belongs to the 2D Ising universality class, can be found in [114]. The two-dimensional case is interesting for several reasons: first, the isothermal condition could probably be realized here most easily experimentally by coupling the fluid to a heat-absorbing substrate. Second, the scaling arguments of sec. II suggest that the fluctuation contributions of various nonlinearities grow around a dimension of $d = 2$. As such effects are difficult to assess analytically, numerical simulations can provide useful insights and are complementary in this case.

A. Setup

Parameters of our LB simulations are chosen as in [114], a typical setup at the critical point being $r = -4.8 \times 10^{-5}$, $u = 2.8 \times 10^{-2}$ and $\kappa = 9.6 \times 10^{-5}$. This choice leads to a mean-field interface width of $\simeq 2$ l.u. and is expected to ensure reliable results on the fluctuation dynamics [114, 115]. The noise temperature is set to $k_B T = 10^{-7}$ and the bare bulk and shear viscosities to $\nu_b = \nu_s = 0.04/3$. Quantitatively similar results have been obtained also for other parameter combinations. Simulation boxes are of size $L \times L = 256^2$, except for Figs. 5 and 6c, where $L \times L = 128^2$. All simulation results reported in the paper are obtained with a standard LB implementation, where the viscous stress consists of terms of the form $\nu \rho \partial_\alpha u_\beta$, i.e., the dynamic viscosities depend on ρ . In a few cases it has been checked, by using an implementation where the ρ -dependence of the dynamic viscosities is eliminated, that results are not affected by this LB specific peculiarity. Besides, due to requirements of numerical stability, relative density fluctuations $\delta\rho/\rho_0$ in our simulations are on average well below a few percent, thus an approximation $\rho \simeq \rho_0$ is warranted. Due to the multiplicative nature of the renormalization of the relaxation rate, the specific values of the viscosities are not important. They do, however, influence the extension of the overdamped acoustic regime and the crossover from mean-field to the expected model-A critical behavior. While a small longitudinal viscosity leads to a more rapid equilibration of the order parameter, it also shifts the onset of the overdamped regime to smaller wavenumbers. In consequence, larger simulation boxes would be required to reduce the residual speed of sound at the critical point sufficiently. Furthermore, a large value of c_s can significantly affect the long-time decay of the order-parameter correlation function, which can be misinterpreted as caused by a larger viscosity. In order to diminish these and other undesired finite-size effects, the lowest k -modes are usually excluded from the analysis of our results. To eliminate effects of lattice anisotropy (cf. [116]), all wavenumber-dependent quantities shown in the plots are computed as an average over the Cartesian axes of the Fourier plane.

The theoretically predicted logarithmic divergence of the viscosities in 2D due to the convective nonlinearity [84–87] is difficult to observe and requires either very long simulation times or large simulation boxes (cf. [117]). Indeed, since the effect is proportional to $k_B T \log L$ [55], it is expected to be below the threshold of statistical accuracy for the present setup.

B. Results

1. Order parameter

Fig. 4a shows the dynamic structure factor $C(k, t)$ at the critical point for different wavenumbers k as obtained from our simulations. The exponential decay of $C(k, t)$ is clearly seen in the semi-logarithmic plot. According to the dynamic scaling hypothesis, $C(k, t) = k^{-2+\eta} C((k\xi)^{-1}, k^z t)$; hence, sufficiently close to the critical point, where $(k\xi)^{-1}$ is small, the dynamic critical index z can be determined by plotting $C(k, t)/C(k, 0)$ versus the rescaled time $k^z t$, testing different values of z until a complete data collapse is achieved. This is done in Fig. 4b, from which we infer a value of $z \simeq 2.25 \pm 0.1$. For comparison, the insets demonstrate that, when rescaling the data with a significantly larger or smaller value of z , the data collapse remains incomplete.

Alternatively to the rescaling procedure, the dynamic critical index can be more directly determined from the relaxation rate $\Gamma(k)$, which can be obtained by fitting an exponential decay [eq. (38)] to the dynamic structure factor. The assumption of an exponential relaxation is well satisfied in the overdamped regime, after neglecting the short-time, non-exponential part of $C(k, t)$ caused by a finite residual speed of sound. In Fig. 4c, the so obtained relaxation rate is plotted against the wavenumber in a double-logarithmic representation. At small wavenumbers, the expected power-law behavior $\Gamma \propto k^z$ is clearly seen. A numerical fit yields a value of the exponent of $z \simeq 2.2 \pm 0.2$, which agrees well with the value obtained above by rescaling the structure factor data.

Within the error margins, the value of z extracted from the simulations thus clearly shows that the dynamic critical index is significantly increased over its mean-field ($z = 2$) or van Hove ($z = 1.75$) value. Moreover, it agrees reasonably well with the theoretical predictions based on pure model-A-type critical behavior [eq. (65)]. Note that the obtained value of z in principle also depends on the range of wavenumbers considered. The deviation from a pure power-law at larger wavenumbers might be caused by the general wavenumber-dependence of the LB transport coefficients [118, 119] or the influence of other nonlinearities in the model that overwhelm the leading order critical divergences. For $k \gtrsim 1$ also the discrete nature of the lattice becomes noticeable (see, e.g., [113, 114]). More precise values for z could be obtained by using larger simulation boxes, thereby extending the low- k regime and decreasing the influence of the non-exponential decay of $C(k, t)$ at short times.

In Fig. 5, the behavior of the order-parameter relaxation rate (obtained from exponential fits) is investigated in greater detail for different wavenumbers k and reduced temperatures θ , where $\theta = (r_c - r)/r_c$. As seen in Fig. 5a, the relaxation rate at fixed k first markedly decreases when approaching the critical point ($\theta = 0$), but eventually levels

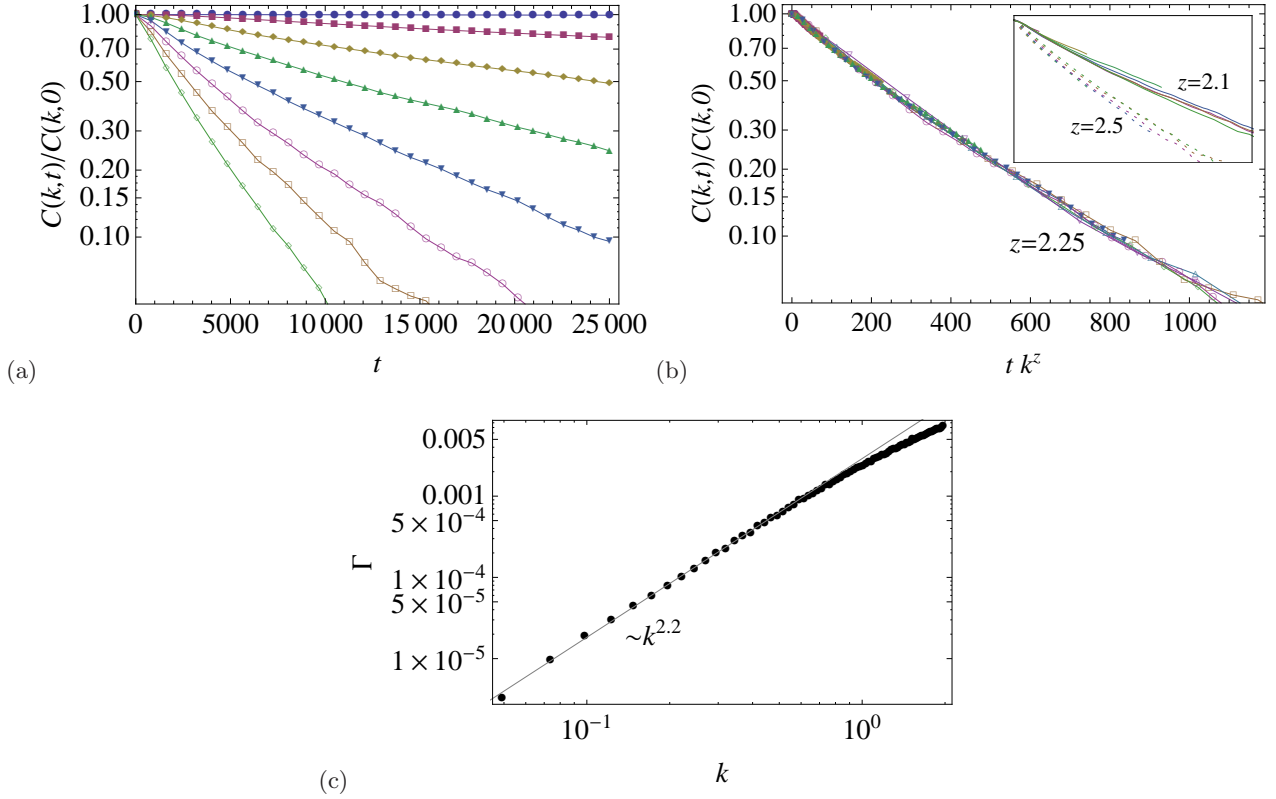


FIG. 4: (a,b) Dynamic structure factor at the critical point: (a) Raw data for the lowest wavenumbers k (increasing from top to bottom). The time is given in lattice units and the lines are drawn as a guide to the eye. (b) Test of the dynamic scaling form of $C(k,t)$. The value of the dynamic critical index z is determined by varying z until all points fall onto a master curve. The inset shows that the collapse is incomplete for z significantly different from 2.25. (c) Relaxation rate Γ at the critical point obtained from exponential fits to the dynamic structure factor for different wavenumbers. The solid line is $\propto k^{2.2}$.

off at a finite value caused by a nonzero speed of sound. Also, the expected temperature dependence $\Gamma \propto \theta^{z\nu}$ with $z\nu \simeq 2.2$ is not observed, but instead a less steep decrease. These effects are well known consequences of the finite system size and can be observed also for static quantities (see [114]). Analogously to statics, finite-size effects can be expected to be much less pronounced when looking directly at the wavenumber dependence of a critical quantity. Indeed, in Fig. 5b it is clearly seen that, when approaching the critical point, Γ smoothly assumes its expected power-law $\propto k^z$. Far above the critical point, order-parameter modes at low k cross over to the propagating regime and a relaxation rate can not be defined anymore.

In Fig. 5c, the effective longitudinal viscosity, $\nu_{lR}(k) = c_{sR}^2(k)/\Gamma(k) = k_B T / [\Gamma(k)C(k)]$, computed from the data of the relaxation rate and static structure factor, is shown. Far above the critical temperature, ν_{lR} assumes its bare value ν_l and is practically independent of wavenumber, while at criticality ($\theta = 0$), the expected power-law divergence $\nu_{lR} \propto k^{-x}$ is reproduced with reasonable accuracy. Note that the critical enhancement is multiplicative and independent of the bare viscosity. Deviations at the lowest k can be attributed to the relatively strong finite-size effects that occur in the static structure factor of the present model [114]: at low k , $C(k)$ appears slightly steeper than the expected $k^{-2+\eta}$ -power law at the critical point, which is reflected in a weaker-than-expected divergence of the longitudinal viscosity.

2. Shear viscosity

Turning to the critical behavior of the shear viscosity, we study here only the contribution from the off-diagonal component of the thermodynamic pressure tensor, $P_{xy} = \kappa(\partial_x \rho)(\partial_y \rho)$, via the Green-Kubo relation, eq. (68). Fig. 6a shows the so obtained temperature-dependence of the fluctuation contribution $\nu_{s,\text{crit}}$ at $k = 0$ in the critical region. The theoretical prediction of eq. (68), represented by the solid curve in Fig. 6a, is found to capture the behavior of the shear viscosity quite well, after correcting for an overall prefactor of $O(1)$. To avoid complications associated with

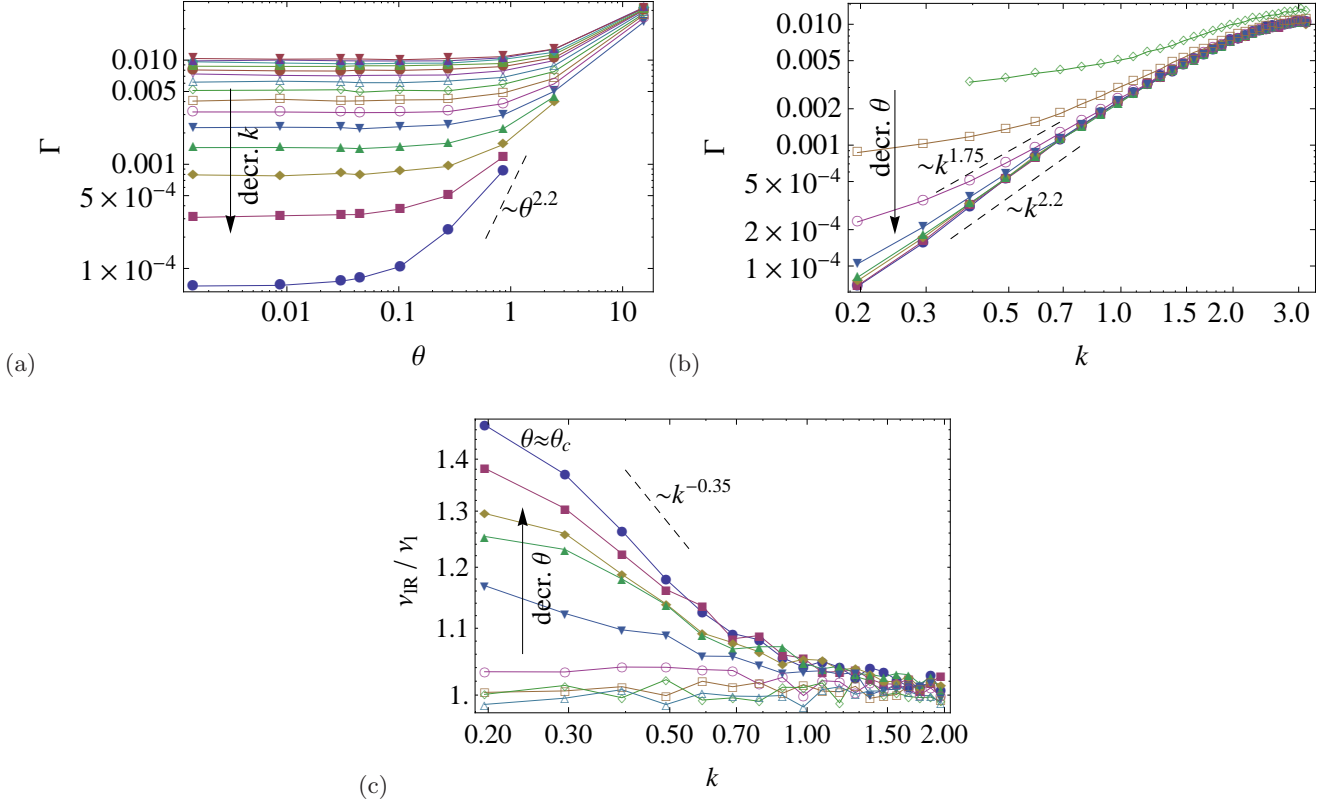


FIG. 5: (a) Dependence of the relaxation rate on the reduced temperature $\theta = (r_c - r)/r_c$ (r is the Landau parameter and r_c its value at the critical point) for different wavenumbers. The expected power-law decrease of Γ (dashed line) is rounded off when approaching the critical temperature due to the finite system size. (b) Wavenumber-dependence of the relaxation rate for different reduced temperatures approaching the critical point from above. Data points in the transition region between the overdamped and propagating acoustic regime are omitted. The power-law $\sim k^{2-\eta} \sim k^{1.75}$ corresponds to the van Hove prediction for Γ , where a wavenumber-independent ν_{lR} is assumed. (c) Effective longitudinal viscosity ν_{lR} (normalized to its bare value ν_l) in dependence of temperature and wavenumber, approaching the critical point from above. Finite-size effects, leading to a weaker-than-expected divergence of ν_{lR} , are noticeable at low k (see text). The lines are drawn as a guide to the eye.

temperature dependent effective critical exponents, mean-field values for η and z have been used in the analytical evaluation of eq. (68), for simplicity. In Fig. 6b, the wavenumber-dependence of the shear viscosity at the critical point obtained from eq. (68) is shown on a double-logarithmic (main plot) and logarithmic-linear (inset) scale. While there appears some logarithmic growth at larger k , the plateau at low k suggests that the shear viscosity stays finite in 2D, in disagreement with the scaling predictions of eq. (68) [130]. The finiteness of the critical shear viscosity can also be seen from its scaling behavior with the system size L (inset to Fig. 6c). Interestingly, $\nu_{s,\text{crit}}$ is found to even decrease with larger L by a power-law with a small exponent of roughly -0.15 . From the finite-size behavior of the shear-stress correlation function, it is inferred that this behavior arises from both a decrease of the shear-stress relaxation time and a decrease of the equal-time autocorrelation of P_{xy} with L (Fig. 6c). We find a similar behavior also slightly away from the critical point, although the effect is less pronounced there. The decay of the shear-stress correlation function is non-exponential and occurs over a shorter timescale than the relaxation of the order parameter.

A possible reason for the disagreement with the critical scaling predictions of eq. (68) might be that, by computing the correlation function of the stress tensor P_{xy} in our simulations, we do not properly take into account the renormalization of κ , which enters here only as a constant numerical prefactor. Indeed, if this effect is neglected in eq. (68), the scaling exponent changes to $z - d - 2\eta < 0$ in 2D, implying a non-divergent $\nu_{s,\text{crit}}$. An alternative method to determine the effective shear viscosity would be to compute the transverse current correlation function. However, due to the small value of κ , which is a constraint of the present LB model (see [113, 114]), $\nu_{s,\text{crit}}$ remains orders of magnitude below its bare value ν_s . Thus, exceeding computational resources would be necessary to extract the fluctuation contribution to the shear viscosity obtained from a correlation function. Further numerical investigation of the shear viscosity in a two-dimensional isothermal fluid using alternative simulation methods are thus desirable.

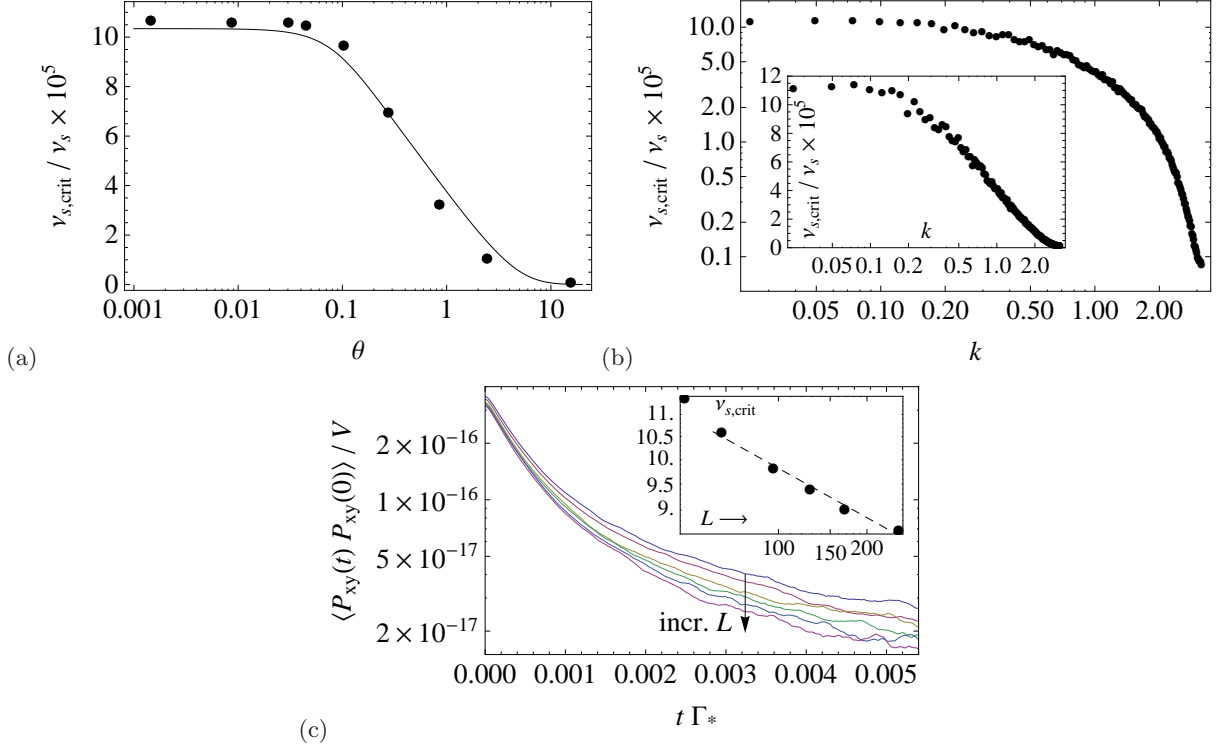


FIG. 6: (a) Critical fluctuation contribution to the shear viscosity in dependence of the reduced temperature. The data (filled symbols) is obtained from simulations using the Green-Kubo relation (68) at $k = 0$. The solid curve represents the theoretical prediction of eq. (68). (b) Wavenumber-dependence of the critical shear viscosity (at $\theta = 0$) obtained from eq. (68), plotted in double-logarithmic representation. For comparison, the same data is plotted in the inset in log-linear scale. (c) Finite-size behavior of the shear stress correlation function (normalized by the system volume $V = L^2$) and the critical fluctuation contribution to the shear viscosity, $\nu_{s,\text{crit}}$ (inset). The dashed curve is $\propto L^{-0.15}$. Time is expressed in units of the characteristic order-parameter relaxation time $1/\Gamma_*$.

for future work.

IV. DISCUSSION

In a conventional single-component fluid (model H), the dominant transport mechanism is heat diffusion, while sound waves are decoupled from the order-parameter dynamics [1, 6, 54, 68]. In contrast, under isothermal conditions, heat diffusion is absent and order-parameter fluctuations can relax only via sound waves. Using a mode-coupling approach, it has been argued here that, below four dimensions, the order-parameter dynamics of the critical isothermal fluid is characterized by model-A-type behavior. This means that, at long wavelengths, sound waves are overdamped due to a strongly diverging bulk viscosity, $\nu_l \propto \xi^x$. The relaxation rate, $\Gamma = c_s^2/\nu_l$, scales as ξ^{-z} with a dynamic critical exponent of $z = \gamma/\nu + x = 2 - \eta + x$, where γ/ν represents the contribution from the isothermal speed of sound and $x \approx 1.7\eta$ represents the “non-classical” contribution from the renormalized bulk viscosity. While in model H, the divergence of the kinetic coefficient arises due to the advective coupling to the transverse velocity modes [6, 54], it is due to the nonlinear thermodynamic pressure in the isothermal case. Longitudinal and transverse currents are approximately decoupled for d close to 4 – a property that becomes exact in the linear case. In 2D, our simulations of the fluctuating hydrodynamic equations yield a value of $z \approx 2.2 \pm 0.1$ and $x \approx 0.45 \pm 0.1$, in reasonable agreement with theoretical predictions and Monte-Carlo simulations of model A. The scaling theory predicts the shear viscosity to remain finite for $d > 2$ and weakly diverge by a power-law in two dimensions. This divergence could, however, not be observed within the present simulation approach. The essential differences in the critical dynamics of an isothermal and an ordinary fluid (model H) are collected in Tab. I.

It is interesting to compare the present findings also to the situation in hydrodynamic models of the glass transition [35, 36, 39, 95], where the isothermal compressible Navier-Stokes equations have been investigated in conjunction with a purely Gaussian free energy. There, the density correlation function shows an anomalously slow decay at

low temperatures, accompanied by a strong increase of the bulk viscosity. Quite analogously to the case in critical dynamics, this is a generic mode-coupling effect caused by a nonlinear pressure term. In the case of a supercooled liquid, however, the dominant contribution arises from the quadratic pressure nonlinearity [$r\phi^2$ in eq. (20)], whereas in the critical fluid, this term turns out to be irrelevant due to the smallness of r .

The present model is particularly interesting in the two-dimensional case, where a possible experimental realization of the isothermal condition might be achievable. While the present scaling considerations indicate the divergence of additional contributions to the bulk viscosity beyond the model-A term, our simulation results suggest that the model-A-type critical behavior essentially persists also in 2D, with possible corrections to critical exponents being small, at least. For future work, it will be interesting to treat the isothermal fluid model within a renormalization-group approach and also derive more detailed predictions in the two dimensional case. In order to clarify the critical behavior of the shear viscosity in 2D, alternative simulation methods could be used.

The predictions obtained in this work might be experimentally testable on single-component monolayer films that admit for liquid-vapor-like phase-separation below a critical point [11, 12]. Of course, the present model is highly idealized in that it neglects the possible influence of electrostatic long-range interactions [120–123], friction between fluid and substrate, and hydrodynamic back-coupling [9, 88, 124, 125]. Also, it is assumed that the rate of heat transfer between fluid and substrate is sufficiently large to provide an effective isothermal environment for the critical fluctuations (see, however, [126]). Since the long-wavelength dynamics of a fluid becomes arbitrarily slow upon approaching the critical point, one might expect that even a relatively small thermal coupling will actually be sufficient.

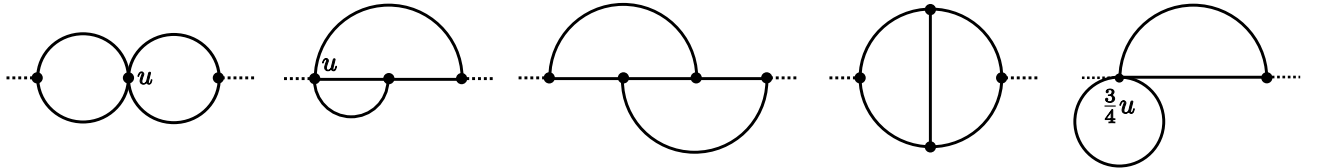
In general, crossover behavior between different dynamic universality classes of a single-component fluid film is expected: in case of negligible friction, model H is obtained for vanishing thermal coupling and, as shown in this work, model A for perfect thermal coupling. In the opposite case of large friction, it is expected that model B (i.e., a purely diffusive order-parameter transport) results [79, 88].

Acknowledgments

We would like to thank R. Adhikari, M. E. Cates, H. W. Diehl, S. May and A. J. Wagner for helpful discussions. Funding from the DFG (Va205/5-2) and the industrial sponsors of ICAMS, the state of North-Rhine Westphalia and the European Commission in the framework of the European Regional Development Fund (ERDF) is gratefully acknowledged. M.G. would also like to thank the EPCC, Edinburgh and the NDSU, Fargo for hospitality.

Appendix A: Further contributions to the self-energy

The contributions to the order-parameter self-energy at two-loop order are diagrammatically represented as:



Here, the unlabeled dots represent the possible couplings r , κ , ν_l , ν_t associated with the three-point vertices. Open circles and arrows (representing correlation or response functions) are understood to be present on some of the internal lines. Also, some diagrams exist with the solid lines replaced by wavy lines representing the transverse current response/correlation functions. Regarding the scaling behavior, however, these modified diagrams need not be explicitly evaluated, since all three-point vertices scale in the same way. Taking into account the proper critical behavior of the couplings, the dynamic part of each diagram is found to scale $\propto \xi^{2-d}$ (up to corrections of exponents of $O(\eta)$) and thus gives negligible contributions to the renormalized viscosity for $d > 2$.

* Electronic address: markus.gross@rub.de

- [1] H. E. Stanley, *Introduction to phase transitions and critical phenomena* (Oxford University Press, 1971).
- [2] P. C. Hohenberg and B. I. Halperin, Rev. Mod. Phys. **49**, 435 (1977).
- [3] J. V. Sengers, in *Supercritical Fluids*, edited by E. Kiran and J. M. H. L. Sengers (Kluwer Academic Publishers, 1994), p. 231.
- [4] R. Folk and G. Moser, J. Phys. A **39**, R207 (2006).

- [5] U. C. Täuber, *Critical Dynamics – A field theory approach to equilibrium and non-equilibrium scaling behavior* (2012), <http://www.phys.vt.edu/~tauber/>.
- [6] A. Onuki, *Phase Transition Dynamics* (Cambridge Univ. Press, 2002).
- [7] D. K. Schwartz, C. M. Knobler, and R. Bruinsma, Phys. Rev. Lett. **73**, 2841 (1994).
- [8] H. A. Stone, Phys. Fluids **7**, 2931 (1995).
- [9] D. K. Lubensky and R. E. Goldstein, Phys. Fluids **8**, 843 (1996).
- [10] G. L. Gaines Jr., *Insoluble Monolayers at Liquid-Gas Interfaces* (Interscience, 1966).
- [11] C. M. Knobler, Science **249**, 870 (1990).
- [12] V. M. Kaganer, H. Moehwald, and P. Dutta, Rev. Mod. Phys. **71**, 779 (1999).
- [13] S. L. Keller and H. M. McConnell, Phys. Rev. Lett. **82**, 1602 (1999).
- [14] L. K. Nielsen, T. Bjornholm, and O. G. Mouritsen, Nature **404**, 352 (2000).
- [15] L. K. Nielsen, T. Bjornholm, and O. G. Mouritsen, Langmuir **23**, 11684 (2007).
- [16] S. L. Veatch and S. L. Keller, Phys. Rev. Lett. **89**, 268101 (2002).
- [17] T. Murtola, T. Rog, E. Falck, M. Karttunen, and I. Vattulainen, Phys. Rev. Lett. **97**, 238102 (2006).
- [18] S. L. Veatch, O. Soubias, S. K. Keller, and K. Gawrisch, Proc. Nat. Acad. Sci. **104**, 17650 (2007).
- [19] A. R. Honerkamp-Smith, P. Cicuta, M. D. Collins, S. L. Veatch, M. den Nijs, M. Schick, and S. L. Keller, Biophys. J. **95**, 236 (2008).
- [20] J. Ehrig, E. P. Petrov, and P. Schuille, New. J. Phys. **13**, 045019 (2011).
- [21] A. R. Honerkamp-Smith, B. B. Machta, and S. L. Keller, Phys. Rev. Lett. **108**, 265702 (2012).
- [22] B. B. Machta, S. L. Veatch, and J. P. Sethna, arXiv:1203.2199 (2012).
- [23] O. G. Mouritsen, *Life - as a Matter of Fat. The Emerging Science of Lipidomics* (Springer, 2005).
- [24] K. Simons and E. Ikonen, Nature **387**, 569 (1997).
- [25] S. L. Veatch and S. K. Keller, Biochim. Biophys. Acta **1746**, 172 (2005).
- [26] J. S. Langer and L. A. Turski, Phys. Rev. A **8**, 3230 (1973).
- [27] O. T. Valls and G. F. Mazenko, Phys. Rev. B **38**, 11643 (1988).
- [28] J. E. Farrell and O. T. Valls, Phys. Rev. B **40**, 7027 (1989).
- [29] J. E. Farrell and O. T. Valls, Phys. Rev. B **42**, 2353 (1990).
- [30] J. E. Farrell and O. T. Valls, Phys. Rev. B **43**, 630 (1991).
- [31] W. R. Osborn, E. Orlandini, M. R. Swift, J. M. Yeomans, and J. R. Banavar, Phys. Rev. Lett. **75**, 4031 (1995).
- [32] A. G. Lamorgese and R. Mauri, Phys. Fluids **21**, 044107 (2009).
- [33] B. U. Felderhoff, Physica A **48**, 541 (1970).
- [34] L. A. Turski and J. S. Langer, Phys. Rev. A **22**, 2189 (1980).
- [35] S. P. Das, G. F. Mazenko, S. Ramaswamy, and J. J. Toner, Phys. Rev. Lett. **54**, 118 (1985).
- [36] S. P. Das and G. F. Mazenko, Phys. Rev. A **34**, 2265 (1986).
- [37] T. R. Kirkpatrick and J. C. Nieuwoudt, Phys. Rev. A **33**, 2651 (1986).
- [38] T. R. Kirkpatrick and J. C. Nieuwoudt, Phys. Rev. A **33**, 2658 (1986).
- [39] S. P. Das, *Statistical physics of liquids at freezing and beyond* (Cambridge Univ. Press, 2011).
- [40] L. Canet and H. Chate, J. Phys. A.: Math. Theor. **40**, 1937 (2007).
- [41] A. S. Krinitsyn, V. V. Prudnikov, and P. V. Prudnikov, Th. Math. Phys. **147**, 561 (2006).
- [42] E. D. Siggia, B. I. Halperin, and P. C. Hohenberg, Phys. Rev. B **13**, 2110 (1976).
- [43] H. C. Burstyn and J. V. Sengers, Phys. Rev. Lett. **45**, 259 (1980).
- [44] H. C. Burstyn and J. V. Sengers, Phys. Rev. A **25**, 448 (1982).
- [45] R. F. Berg, M. R. Moldover, and G. A. Zimmerli, Phys. Rev. Lett. **82**, 920 (1999).
- [46] R. F. Berg, M. R. Moldover, and G. A. Zimmerli, Phys. Rev. E **60**, 4079 (1999).
- [47] H. Hao, R. A. Ferrell, and J. K. Bhattacharjee, Phys. Rev. E **71**, 021201 (2005).
- [48] A. Onuki, Phys. Rev. E **55**, 403 (1997).
- [49] P. M. Chaikin and T. C. Lubensky, *Principles of Condensed Matter Physics* (Cambridge, 1995).
- [50] K. Kawasaki, Ann. Phys. **61**, 1 (1970).
- [51] B. I. Halperin, P. C. Hohenberg, and E. D. Siggia, Phys. Rev. Lett. **32**, 139 (1974).
- [52] L. P. Kadanoff and J. Swift, Phys. Rev. **166**, 166 (1968).
- [53] L. van Hove, Phys. Rev. **95**, 249 (1954).
- [54] K. Kawasaki, in *Phase Transitions and Critical Phenomena*, edited by C. Domb and M. S. Green (Academic Press, 1976), vol. 5A, p. 165.
- [55] G. F. Mazenko, *Nonequilibrium Statistical Mechanics* (Wiley-VCH, 2006).
- [56] J. K. Bhattacharjee and S. Bhattacharyya, *Non-Linear Dynamics Near and Far from Equilibrium* (Springer, 2007).
- [57] T. Ohta and K. Kawasaki, Prog. Theor. Phys. **55**, 1384 (1976).
- [58] T. Ohta and K. Kawasaki, Phys. Lett. **30**, 325 (1969).
- [59] D. M. Kroll and J. M. Ruhland, Phys. Lett. **80A**, 45 (1980).
- [60] D. M. Kroll and J. M. Ruhland, Phys. Rev. A **23**, 371 (1981).
- [61] R. Dengler and F. Schwabl, Europhys. Lett. **4**, 1233 (1987).
- [62] R. Dengler and F. Schwabl, Z. Phys. B **69**, 327 (1987).
- [63] R. Folk and G. Moser, J. Low. Temp. Phys. **99**, 11 (1995).
- [64] R. Folk and G. Moser, Phys. Rev. E **57**, 683 (1998).
- [65] R. Folk and G. Moser, Phys. Rev. E **57**, 705 (1998).

- [66] G. Flossmann, R. Folk, and G. Moser, Phys. Rev. E **60**, 779 (1999).
- [67] L. T. Adzhemyan, A. N. Vasil'ev, and A. V. Serdyukov, JETP **87**, 934 (1998).
- [68] J. K. Bhattacharjee, U. Kaatz, and S. Z. Mirzaev, Rep. Prog. Phys. **73**, 066601 (2010).
- [69] L. D. Landau and E. M. Lifshitz, *Fluid Mechanics* (Pergamon, 1959).
- [70] J.-P. Hansen and I. R. McDonald, *Theory of Simple Liquids* (Academic Press, 2006), 3rd ed.
- [71] J. P. Boon and S. Yip, *Molecular Hydrodynamics* (McGraw-Hill, 1980).
- [72] S. K. Das, M. E. Fisher, J. V. Sengers, J. Horbach, and K. Binder, Phys. Rev. Lett. **97**, 025702 (2006).
- [73] S. K. Das, J. Horbach, K. Binder, M. E. Fisher, and J. V. Sengers, J. Chem. Phys. **125**, 024506 (2006).
- [74] K. Jagannathan and A. Yethiraj, Phys. Rev. Lett. **93**, 015701 (2004).
- [75] A. Chen, E. H. Chimowitz, S. De, and Y. Shapir, Phys. Rev. Lett. **95**, 255701 (2005).
- [76] T. Hamanaka, R. Yamamoto, and A. Onuki, Phys. Rev. E **71**, 011507 (2005).
- [77] S. Roy and S. K. Das, EPL **94**, 36001 (2011).
- [78] S. A. Casalnuovo, R. C. Mockler, and W. J. O'Sullivan, Phys. Rev. Lett. **48**, 939 (1982).
- [79] S. A. Casalnuovo, R. C. Mockler, and W. J. O'Sullivan, Phys. Rev. A **29**, 257 (1984).
- [80] M. Calvo and R. A. Ferrell, Phys. Rev. A **31**, 2570 (1985).
- [81] M. Calvo, Phys. Rev. A **31**, 2588 (1985).
- [82] J. K. Bhattacharjee, Phys. Rev. Lett. **77**, 1524 (1996).
- [83] W.-B. Zhang, X.-W. Zou, H.-Y. Liu, Z.-Z. Jin, and D.-C. Tian, Phys. Lett. A **272**, 408 (2000).
- [84] Y. Pomeau, Phys. Rev. A **5**, 2569 (1971).
- [85] Y. Pomeau and P. Resibois, Phys. Rep. **19**, 63 (1975).
- [86] D. Forster, D. R. Nelson, and M. J. Stephen, Phys. Rev. Lett. **36**, 867 (1976).
- [87] D. Forster, D. R. Nelson, and M. J. Stephen, Phys. Rev. A **16**, 732 (1977).
- [88] S. Ramaswamy and G. F. Mazenko, Phys. Rev. A **26**, 1735 (1982).
- [89] B. Kim and G. F. Mazenko, J. Stat. Phys. **64**, 631 (1991).
- [90] A. J. M. Yang, P. D. Fleming III, and J. H. Gibbs, J. Chem. Phys. **64**, 3732 (1976).
- [91] R. Evans, Adv. Phys. **28**, 143 (1979).
- [92] J. Lowengrub and L. Truskinovsky, Proc. R. Soc. Lond. A **454**, 2617 (1988).
- [93] D. Jasnow and J. Vinals, Phys. Fluids **8**, 660 (1996).
- [94] D. M. Anderson, G. B. McFadden, and A. A. Wheeler, Annu. Rev. Fluid. Mech. **30**, 139 (1998).
- [95] K. Kawasaki, Transport Theory and Statistical Physics **24**, 755 (1995).
- [96] I. Staroselsky, V. Yakhot, S. Kida, and S. A. Orszag, Phys. Rev. Lett. **65**, 171 (1990).
- [97] G. F. Mazenko and Y. Yeo, J. Stat. Phys. **74**, 1017 (1994).
- [98] R. Folk, H. Iro, and F. Schwabl, Phys. Rev. B **20**, 1229 (1979).
- [99] F. Schwabl, J. Stat. Phys. **39**, 719 (1985).
- [100] S.-K. Ma, *Modern Theory of Critical Phenomena* (Westview Press, 1976).
- [101] K. Kawasaki and J. D. Gunton, Phys. Rev. B **13**, 4658 (1976).
- [102] J. Luettmer-Strathmann, J. V. Sengers, and G. A. Olchowy, J. Chem. Phys. **103**, 7482 (1995).
- [103] S.-K. Ma and G. F. Mazenko, Phys. Rev. B **11**, 4077 (1975).
- [104] R. A. Ferrell and J. K. Bhattacharjee, J. Low. Temp. Phys. **36**, 165 (1979).
- [105] P. Kopietz, L. Bartosch, and F. Schuetz, *Introduction to the Functional Renormalization Group* (Springer, 2010).
- [106] B. I. Halperin, P. C. Hohenberg, and S.-K. Ma, Phys. Rev. Lett. **29**, 1548 (1972).
- [107] B. I. Halperin, P. C. Hohenberg, and S.-K. Ma, Phys. Rev. B **10**, 139 (1974).
- [108] B. I. Halperin, P. C. Hohenberg, and S.-K. Ma, Phys. Rev. B **13**, 4119 (1976).
- [109] M. P. Nightingale and H. W. J. Blöte, Phys. Rev. Lett. **76**, 4548 (1996).
- [110] J. Rogiers and J. O. Indekeu, Phys. Rev. B **41**, 6998 (1990).
- [111] M. J. Dunlavy and D. Venus, Phys. Rev. B **71**, 144406 (2005).
- [112] R. Perl and R. A. Ferrell, Phys. Rev. A **6**, 2358 (1972).
- [113] M. Gross, R. Adhikari, M. E. Cates, and F. Varnik, Phys. Rev. E **82**, 056714 (2010).
- [114] M. Gross and F. Varnik, Phys. Rev. E **85**, 056707 (2012).
- [115] A. J. Wagner and C. M. Pooley, Phys. Rev. E **76**, 045702(R) (2007).
- [116] S. P. Thampi, S. Ansumali, R. Adhikari, and S. Succi, arXiv:1202:3299 (2012).
- [117] U. Frisch, D. d'Humieres, B. Hasslacher, P. Lallemand, Y. Pomeau, and J.-P. Rivet, Complex Systems **1**, 649 (1987).
- [118] O. Behrend, R. Harris, and P. B. Warren, Phys. Rev. E **50**, 4586 (1994).
- [119] P. Lallemand and L.-S. Luo, Phys. Rev. E **61**, 6546 (2000).
- [120] H. M. McConnell, Annu. Rev. Phys. Chem. **42**, 171 (1991).
- [121] R. Folk and G. Moser, Phys. Rev. E **49**, 3128 (1994).
- [122] K. Binder and E. Luijten, Phys. Rep. **344**, 179 (2001).
- [123] S. V. Belim, J. Exp. Theor. Phys. **98**, 745 (2004).
- [124] J. C. Alexander, A. J. Bernoff, E. K. Mann, J. A. M. Jr, J. B. Wintersmith, and L. Zou, J. Fluid Mech. **571**, 191 (2007).
- [125] M. Haataja, Phys. Rev. E **80**, 020902(R) (2009).
- [126] J. Griesbauer, A. Wixforth, and M. F. Schneider, Biophys. J. **97**, 2710 (2009).
- [127] This expression for the speed of sound holds only in the supercritical regime. Below the critical point ($r < 0$), the nonlinear terms provide an additional contribution, so that c_s^2 is positive in each bulk phase.
- [128] More generally, one would expect that $c_{sR}(\mathbf{k}) = k_B T / C(\mathbf{k})$ for arbitrary k , as a consequence of an fluctuation-response

relation like eq. (31). Due to the presence of the $1/\rho$ -nonlinearity, however, there is no simple FDT like eq. (30) connecting the full correlation and response function in the compressible fluid, except in the small- k limit [36, 39]. An FDT can be proven for the nonlinear oscillator eq. (26) if the $1/\rho$ -nonlinearity is neglected, see [98]

- [129] Note that the conserved nature of the fluid order parameter (density) becomes noticeable only at early times, where the correlation function decays non-exponentially and the dynamics deviates from pure model-A behavior.
- [130] Although the shear-viscosity at $k = 0$ when plotted against reduced temperature (Fig. 6a) exhibits an extended plateau towards $\theta \rightarrow 0$ as well, this effect can not be unambiguously attributed to the non-divergent nature of $\nu_{s,\text{crit}}$, as finite-size effects are expected to contribute significantly here (cf. Fig. 5a,b, where a similar effect is seen for the relaxation rate).